Earth and Planetary Science Letters 569 (2021) 117037

Contents lists available at ScienceDirect

Earth and Planetary Science Letters

www.elsevier.com/locate/epsl

Seismogenic and tremorgenic slow slip near the stability transition of frictional sliding

Shiying Nie *, Sylvain Barbot

University of Southern California, Department of Earth Sciences, United States of America

ARTICLE INFO

Article history:
Received 24 November 2020
Received in revised form 20 April 2021
Accepted 1 June 2021
Available online xxxx
Editor: R. Bendick

Keywords:
slow slip events
tremors
earthquake physics

ABSTRACT

Slow-slip events and tremors occur below the seismogenic zone of major plate boundaries. While the physics of aseismic slow-slip events is relatively well understood, the mechanics of seismogenic slow slip remains elusive because the conditions leading to slow or fast ruptures are thought to be mutually exclusive. Here, we explore fault dynamics in the parametric space of frictional conditions to show that seismogenic slow-slip events are the natural behavior of homogeneous faults, as long as the velocity dependence approaches velocity neutral with a small characteristic nucleation size. Tremors can originate from rapid bursts of slow earthquakes that are triggered as the slow-slip rupture spreads over small-scale asperities. The near velocity-neutral conditions explain the underlying mechanics of collocated slow and fast slip of seismogenic slow-slip events commonly found below the seismogenic zone. The presence of material heterogeneity may explain the spatio-temporal clustering and migration features of tremor activity.

1. Introduction

Fault dynamics involve a wide range of rupture styles from slow-slip events to large earthquakes. However, slow-slip events are often associated with so-called slow earthquakes. The slow earthquake family includes several types of events based on their frequency and characteristics. Events identified in a frequency band higher than 1 Hz are called low-frequency earthquakes, and those found in the 0.01-0.10 Hz bandwidth are called very-low-frequency earthquakes (Masuda et al., 2020). Furthermore, tremors are distinguished from low-frequency earthquakes based on their seismic wave phases. While low-frequency earthquakes have identifiable P or S wave arrivals, tremors have no distinct body wave arrivals. Tremors are sometimes interpreted as a burst of low-frequency earthquakes (McCausland et al., 2005; Shelly et al., 2007b).

Concurrent slow-slip events and slow earthquakes have been found in several subduction zones (Fig. 1), including Cascadia (Dragert et al., 2001; Rogers and Dragert, 2003; Peng and Rubin, 2016), the Aleutian (Rousset et al., 2019b), the Nankai Trough in Japan (Shelly et al., 2006; Yokota et al., 2016; Shiraishi et al., 2020), the Mid-American Trench in Mexico (Kostoglodov et al., 2003; Frank et al., 2013), and Hikurangi in New Zealand (Kim et al., 2011; Todd et al., 2018). Concurrent slow-slip events and tremors are also found at major strike-slip faults, for example at the San Andreas Fault near Parkfield (Nadeau and Dolenc, 2005; Shelly, 2010; Rousset et al., 2019a) and at the Alpine Fault in New Zealand (Chamberlain et al., 2014; Wech et al., 2012).

Slow-slip events and slow earthquakes represent widely different rupture behaviors. Slow earthquakes last minutes to hours and radiate broadband seismic signals up to 10 Hz. In contrast, slow-slip events have a slip velocity only slightly higher than background relative plate motion and last from days to months. Despite their different characteristics, the two phenomena are mechanically coupled, as most slow-slip events are accompanied by slow earthquakes with temporal and spatial correlation (e.g. Beroza and Ide, 2011). The intensity of tremor activity varies among slow-slip events. For example, the gap between the seismogenic zone and short-term tremorgenic slow-slip area at the Nankai (Takagi et al., 2016; Obara and Kato, 2016; Gao and Wang, 2017) and Mexico (Zigone et al., 2012; Peng and Rubin, 2017) subduction zones are filled with long-term, less seismically active slow-slip events.

Dominantly aseismic slow-slip events are a relatively well-understood phenomenon through numerical simulations. Slow-slip events may occur due to conditional stability when rupture nucleation is limited by fault width (Liu and Rice, 2005), or through enhanced stability by dilatant strengthening (Segall et al., 2010), by restrengthening at high slip speed (Shibazaki and Shimamoto, 2007; Matsuzawa et al., 2010; Im et al., 2020) or by spontaneous thermal instabilities arising from a positive feedback between shear heating and temperature-weakening friction

* Corresponding author.
E-mail address: shiyingn@usc.edu (S. Nie).

https://doi.org/10.1016/j.epsl.2021.117037
0012-821X/

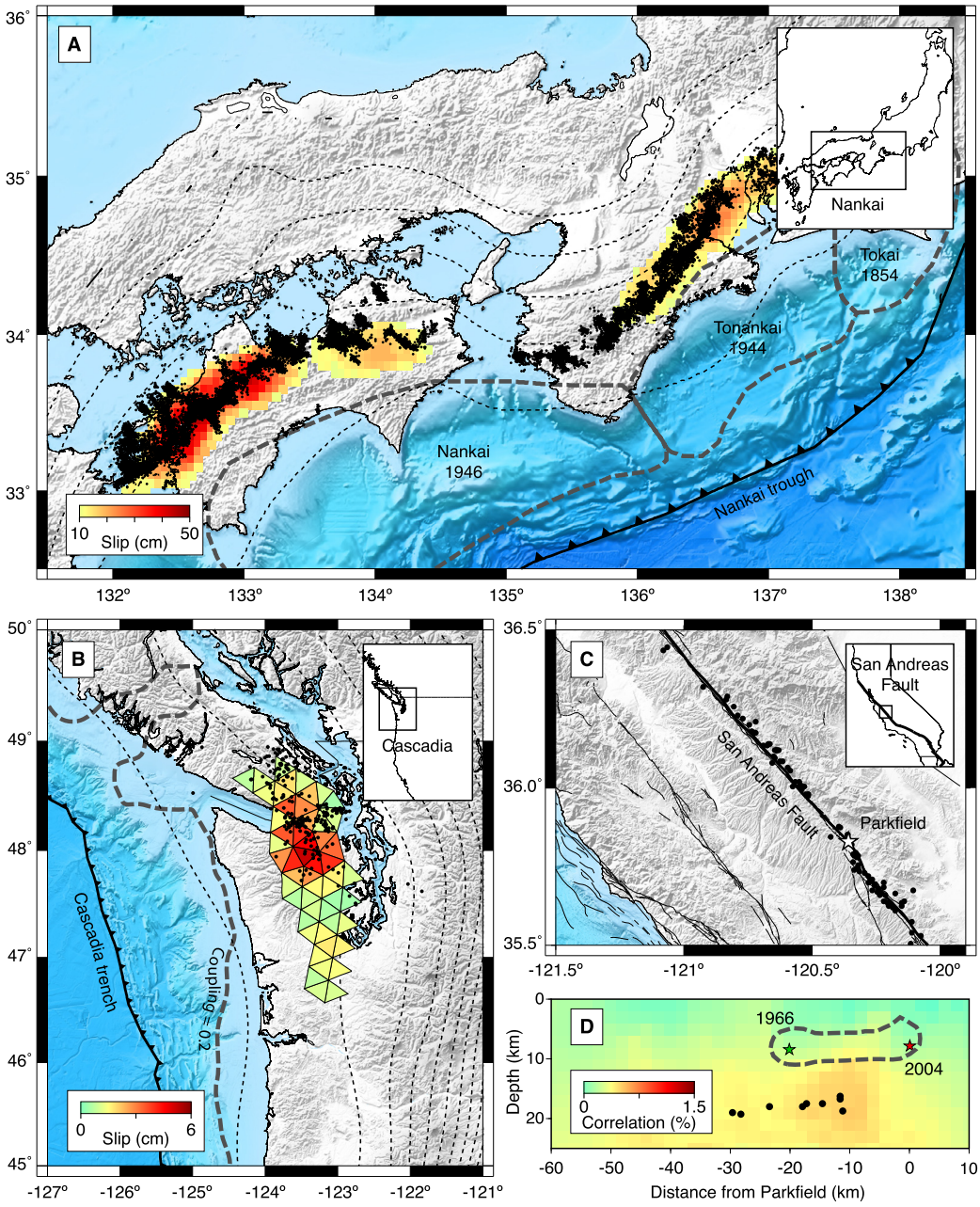

Fig. 1. Concurrence of slow-slip events and slow earthquakes at major plate boundaries. A) Slow-slip events (Nishimura et al., 2013) and tremors (NIED catalogue) in 2012, and rupture area (thick dashed line) of historical large earthquakes (Obara and Kato, 2016) at the Nankai Trough, Japan. B) Collocated tremors (Idehara et al., 2014) and slow-slip (Schmidt and Gao, 2010) at the Cascadia subduction zone. The seismogenic zone is situated above the region of high geodetic coupling (thick dashed line from Michel et al., 2019). The thin dash lines in A) and B) correspond to the USGS Slab2 model (Hayes et al., 2018). C) Distribution of low-frequency earthquakes along the San Andreas Fault (Shelly and Hardebeck, 2010). D) Low-frequency earthquakes and correlation with surface geodetic measurements (Rousset et al., 2019a). The seismogenic region (thick dashed line from Barbot et al., 2012) surrounds the hypocenters of the 1966 (green star) and 2004 (red star) earthquakes. (For interpretation of the colors in the figures, the reader is referred to the web version of this article.)

(Wang and Barbot, 2020). Slow-slip events may also emerge near the brittle-ductile transition due to the stabilizing effect of viscoelastic flow (Goswami and Barbot, 2018; Biemiller and Lavier, 2017; Tong and Lavier, 2018). The circulation of fluids along the fault may also trigger slow slip (Bernaudin and Gueydan, 2018; Cruz-Atienza et al., 2018; Bhattacharya and Viesca, 2019).

In contrast, the physics underlying coincident slow slip and slow earthquakes is unresolved because the conditions leading to slow or fast slip are thought — incorrectly — to be mutually exclusive. Sustained sequences of slow and fast ruptures on the same asperity have been obtained under specific conditions (e.g., Veedu and Barbot, 2016; Romanet et al., 2018; Veedu et al., 2020), but the two rupture styles do not occur within the same event. Recent studies cover the joint occurrence of slow and fast ruptures (Barbot, 2019b; Shi et al., 2020), but this phenomenon has only been described briefly. Other works explore the emergence of seismic events during creep or slow slip invoking a heterogeneous rock matrix in the fault zone (Lavier et al., 2020) or lateral variations of frictional properties along the fault (Dublanchet et al., 2013). Elucidating the physics of concurrent tremor and slow slip still constitutes a major challenge in tectonophysics (Jolivet and Frank, 2020).

In this study, we argue that coincident slow slip and slow earthquakes are the natural response of faults near the transition

between velocity-weakening and velocity-strengthening properties. This condition is universally found below the seismogenic zone and can be accomplished by a wide range of frictional properties. We present numerical simulations of the seismic cycle that produce recurring slow-slip events while resolving the simultaneous nucleation, rupture propagation, and arrest of triggered slow earthquakes in a continuum. The model provides a source mechanism for slow slip and slow earthquakes and explains the occurrence of this phenomenon below the seismogenic zone at many subduction zones and in a continental transform setting. Further, we explain the generation of tremors by the presence of small-scale asperities that are triggered during the passage of a slow-slip rupture front. The model helps us understand the clustering, stationarity, and rapid migration of tremors.

In the next section, we describe the physical assumptions and the numerical method. We then describe the parametric domains leading to aseismic or seismogenic slow-slip events using a homogeneous asperity model. Finally, we present seismic cycle simulations of tremorgenic slow-slip events in the presence of small-scale frictional heterogeneities. We produce synthetic geodetic time series and seismic waveforms that bear resemblance with observed slow-slip events, low-frequency earthquakes, and tremors for natural faults. Our results help understand why seismogenic slow-slip events occur in a wide range of conditions, the variability of tremorgenic potential being controlled by the degree of material heterogeneity of the host fault.

2. Physical assumptions and modeling method

Concurrent slow-slip events and tremors occur in various tectonic settings, including subduction zones and continental transforms. Since slow-slip events often occupy a fault area with a large aspect ratio, we conduct numerical simulations of the seismic cycle using a two-dimensional approximation. The anti-plane strain and in-plane strain approximations are most relevant for strike-slip and thrust faulting, respectively, but fault dynamics in these conditions are similar, only differing by the stiffness of asperities, which depends on Poisson's ratio for mode II cracks. We proceed with the anti-plane strain approximation, but the results remain relevant for in-plane strain given a systematic change of parameters that affects the nucleation size.

We conduct numerical simulations of fault dynamics based on a physics-based rate- and state-dependent friction law, building on a long legacy of studies that describe a wide range of faulting behaviors during seismic cycles, including slow-slip events, fast ruptures, and aperiodic seismic cycles (e.g., Tse and Rice, 1986; Liu and Rice, 2007; Lapusta et al., 2000; Barbot et al., 2012; Wu and Chen, 2014; Qiu et al., 2016; Ong et al., 2019; Barbot, 2020, and references therein). We consider the multiplicative form of a friction constitutive law (Barbot, 2019a) in isothermal conditions given by

$$\tau = \mu_0 \bar{\sigma} \left(\frac{V}{V_0} \right)^{\frac{a}{\mu_0}} \left(\frac{\theta V_0}{L} \right)^{\frac{b}{\mu_0}} , \tag{1}$$

where μ_0 represents the static friction coefficient, V_0 is a reference velocity, and a and b are power exponents for the rate and state dependence of the frictional resistance, respectively. Velocity-weakening at steady state is obtained for $a - b < 0$ and velocity-strengthening for $a - b > 0$. The effective normal stress $\bar{\sigma}$ is affected by the pore-fluid pressure as $\bar{\sigma} = \sigma - p_f$, where σ is the normal traction and p_f is the pore-fluid pressure in the fault zone. The frictional resistance is modulated by the age of contact following the aging law (Ruina, 1983) in isothermal conditions, given by

$$\dot{\theta} = 1 - \frac{V\theta}{L} , \tag{2}$$

where L represents a characteristic weakening distance and θ represents the age of contact.

Slow-slip events are often associated with elevated pore-fluid pressure (e.g., Gao and Wang, 2017), revealed by an elevated ratio of compressional to shear wave speeds in major plate boundaries, including Cascadia (Audet et al., 2009), the Nankai Trough (Kodaira et al., 2004), Hikurangi (Bell et al., 2010), Mexico (Frank et al., 2015), and the San Andreas Fault (Ozacar and Zandt, 2009). The direct effect of high pore-fluid pressure in the fault zone is to decrease the effective normal stress (Song et al., 2009), compatible with the exceedingly small stress drop of slow-slip events (Nanjundiah et al., 2020). We incorporate this effect by considering near-lithostatic pore-fluid pressure, resulting in an effective normal stress of 20 MPa for all models considered.

The wide spectrum of rupture styles that develop during seismic cycles is controlled by the frictional and geometrical properties of a fault. These parameters can be combined into dominantly two non-dimensional parameters that, within realistic bounds, exert a strong control on rupture dynamics (Barbot, 2019b). The Dieterich-Ruina-Rice number

$$R_u = \frac{(b-a)\bar{\sigma}}{G} \frac{W}{L} , \tag{3}$$

incorporates the asperity size W, the rate dependence at steady state $(a - b)$, the characteristic weakening distance, the rigidity G of the host rocks, and the effective normal stress and controls the complexity of fast rupture cycles (Cattania, 2019). The other number

$$R_b = \frac{b-a}{b} \tag{4}$$

controls the ratio of dynamic to static stress drops (Gabriel et al., 2012) and reflects the relative importance of the evolutionary effects. The development of instabilities within the framework of rate- and state-dependent friction has been typically associated with a critical stiffness or a ratio of nucleation size to asperity size (Ruina, 1983; Rice, 1983; Rice and Ruina, 1983). Accordingly, numerical models of slow-slip events are often obtained using a small ratio of the seismogenic width to a characteristic nucleation size, i.e., $R_u \sim 1$ (e.g., Liu and Rice, 2005, 2007; Rubin, 2008; Liu and Rice, 2009; Wei et al., 2013), unless different mechanical behaviors are assumed, but the role of the R_b number has been largely overlooked. Slow-slip events can in fact occur for a wide range of frictional properties as R_b approaches zero from above (Rubin, 2008; Wu and Chen, 2014; Barbot, 2019b). In addition, consideration of nonlinear stability analysis (Viesca, 2016b,a) indicates the apparition of new Hopf bifurcations during rupture nucleation when the velocity-weakening friction properties converge towards velocity neutral, i.e., as R_b approaches zero.

We develop quasi-dynamic simulations of seismic cycles with adaptive time steps to explore a broad spectrum of seismic and aseismic activity while maintaining high numerical accuracy. Adaptive time-stepping is key to resolve the enormous range of time scales relevant to slow slip and slow earthquakes. We use the spectral boundary-integral method with shared memory parallelism to resolve the stress interactions during rupture dynamics with great numerical efficiency (Barbot, 2021). For all simulations, we set the fault width as 15 km and the velocity-weakening region extends from 5 to 10 km. We load the fault at a rate of 83 mm/yr or 2.6×10^{-9} m/s, which is typical for a subduction zone setting. For all models considered, the numerical grid size is chosen to resolve the cohesion length

$$L_b = \frac{GL}{b\bar{\sigma}} . \tag{5}$$

Following a convergence test, we choose a grid size smaller than $L_b/4$ for the homogeneous models of Section 3 and of $L_b/15 = 15$ cm for the heterogeneous model of Section 4.

3. Seismogenic slow-slip events

Episodic tremor and slow-slip events often take place between the seismogenic zone and regions of long-term stable sliding (e.g. Obara and Kato, 2016; Gao and Wang, 2017). In a continental setting, the depth extent of the seismogenic zone is controlled by the stability of wet granite or quartz-rich gouge (Blanpied et al., 1991, 1995, 1998) and the top and bottom boundaries of the seismogenic zone correspond to isotherms (Scholz, 1998). This is perhaps best evidenced by the correlation of heat flow and depth of background seismicity in California (Magistrale, 2002; Hauksson, 2011). In a subduction zone setting, the stability transition may also be controlled by regional metamorphism due to the fluid-rich, low-temperature conditions near the subducting slab. Slow-slip events can occur at greater depths than for a continental transform because of the presence of antigorite-rich serpentinite, which is velocity-weakening at and above 450 °C (Okazaki et al., 2013; Okazaki and Katayama, 2015). Mantle rocks are also velocity-weakening at greater temperatures than granitic rocks (Boettcher et al., 2007). Nevertheless, in both continental and subduction settings, the slow-slip events and tremors phenomenon seems to be associated with a stability transition.

Motivated by these observations, we explore the dynamics of a single velocity-weakening asperity in conditions of near-neutral velocity-weakening friction at steady state. We explore the parametric space of frictional parameters to determine the various styles of slow-slip events that may emerge in various physical conditions near the stability transition. While keeping the width of the velocity-weakening region and effective normal stress fixed, we vary the state-dependence power exponent and the characteristic weakening distance to explore the two-dimensional space of non-dimensional parameters R_u and R_b (Fig. 2). We simulate seismic-cycles with R_b ranging from 0.02 to 0.5 and R_u ranging from 0.6 to 220. We show that slow slip within the rate- and state-dependent friction framework can be classified into three parametric sub-domains: creep, aseismic slow-slip events, and seismogenic slow-slip events.

Aseismic slow-slip events emerge when the rupture is limited to the nucleation phase by the boundaries of the velocity-weakening region. They occur for a narrow range of R_u number that depends on the R_b number. For strongly velocity-weakening asperities with $0.2 \leq R_b \leq 1$, aseismic slow-slip events take place for $1 < R_u < 3$. For asperities in near velocity-neutral conditions with $0 < R_b < 0.1$, aseismic slow-slip events take place for the range $5 < R_u < 10$. Waves of partial coupling (Fig. 2b) may propagate for decades with a slip velocity only slightly above and below the background long-term fault slip-rate. This behavior occurs for intermediate values of R_u and R_b and may be important to understand decadal-scale variations in fault sliding velocity.

Seismogenic slow-slip events (Fig. 2f-i) occur in the conditions predicted by Viesca (2016b,a) for $R_b \sim 0$ and $R_u \gg 1$. The chaotic nucleation regime manifests itself in seismic cycles by numerous fast ruptures embedded in longer and larger slow-slip events. The nucleation of seismogenic slow-slip events may be caused by the coalescence of slow-slip rupture fronts, which is consistent with observations from the laboratory (Kaneko and Ampuero, 2011; Fukuyama et al., 2018) and from the Cascadia subduction zone (Bletery and Nocquet, 2020). For this type of event to emerge spontaneously requires near-neutral velocity-weakening friction and a small enough characteristic nucleation size. We limit our simulations to $R_u = 220$ due to the challenges associated with numerical convergence, but the R_u number has virtually no upper bound. We expect that slow-slip events continue to grow in complexity for increasing R_u numbers. In other words, the characteristic weakening distance may be arbitrarily small and still allow seismogenic slow-slip events.

Seismogenic slow-slip events may occur for a wide range of parameters, including virtually arbitrarily small weakening distance, in conditions of near-neutral velocity-weakening properties. These findings help explain the presence of slow-slip events below the seismogenic zone of continental transforms and subduction zones at the broad transition between stick-slip and stable sliding. In addition, the near velocity-neutral regime helps explain the typical association of slow-slip events with slow earthquakes. The remaining unknown is the mechanics of tremor generation.

4. Tremorgenic slow-slip events

Seismogenic slow-slip events represent complex slow ruptures that incorporate slow earthquakes. However, slow-slip events in nature are frequently associated with tremors, a more specific type of seismicity. As tremors do not seem to form spontaneously in homogeneous velocity-weakening asperities, we introduce small-scale asperities within the velocity-weakening region. The presence of small-scale asperities changes the macroscopic rupture behavior, for example, by generating foreshocks and aftershocks in the seismogenic zone (e.g., Dublanchet, 2017; Yabe and Ide, 2018) or by affecting the macroscopic stability of the fault (Skarbek et al., 2012; Luo and Ampuero, 2018). The rupture dynamics depend on the density of small-scale asperities and their physical properties. After exploring various configurations and considering the phase diagram of Fig. 2, we present the details of a single model that exhibits the characteristic features of tremorgenic slow-slip events in nature, such as event duration of the order of months, recurrence times of the order of years, and typical seismo-geodetic signatures.

We simulate seismogenic slow-slip cycles with heterogeneous frictional properties consisting of a matrix of 50 m-wide asperities with $R_b = 0.2$ embedded in a 5 km-wide near-neutral velocity-weakening fault with $R_b = 0.02$ (Fig. 3). The model produces a non-characteristic sequence of seismogenic slow-slip events. Fast sub-events are triggered at the velocity-weakening asperities by the passage of the slow-slip rupture fronts. We identify the fast events using the slip velocity threshold of 0.01 m/s, but these fast events vary in both peak slip velocity and seismic moment. Rapid failure at the asperities disturbs the propagation of the underlying slow-slip events, resulting in multiple secondary slip fronts. Because the location of small-scale asperities is stationary, the triggered slow earthquakes form repeaters within a single slow-slip event and provide markers of the rupture front. The up-dip and down-dip propagation of the rupture front causes reversal migration of slow earthquakes. In addition, most of the fast sub-events occur within slow-slip events and cluster in time (Fig. 4).

We seek to determine the nature of the slow-slip cycle from the point of view of seismo-geodetic observations. We therefore compute geodetic and seismic recordings to reveal whether the fast sub-events represent earthquakes or tremors and whether the deformation is nominally seismic or aseismic. We first compute the geodetic displacement time series for 5.4 years using elastostatic Green's functions for a homogeneous half space with two-dimensional line sources (Okada, 1985). For these calculations, we assume a fault dip angle of 7.1° (Fig. 5a). We remove the long-term displacement accumulation represented by a linear trend to accentuate the dynamic range from the slow-slip events. Long-term deformation associated with slow slip is detected in synthetic geodetic time series (Fig. 5b), with a rapid first phase followed by a gradual recovery to background strain accumulation due to propagation of slow slip into the velocity-strengthening region. The cumulative surface displacement per event is of the order of several

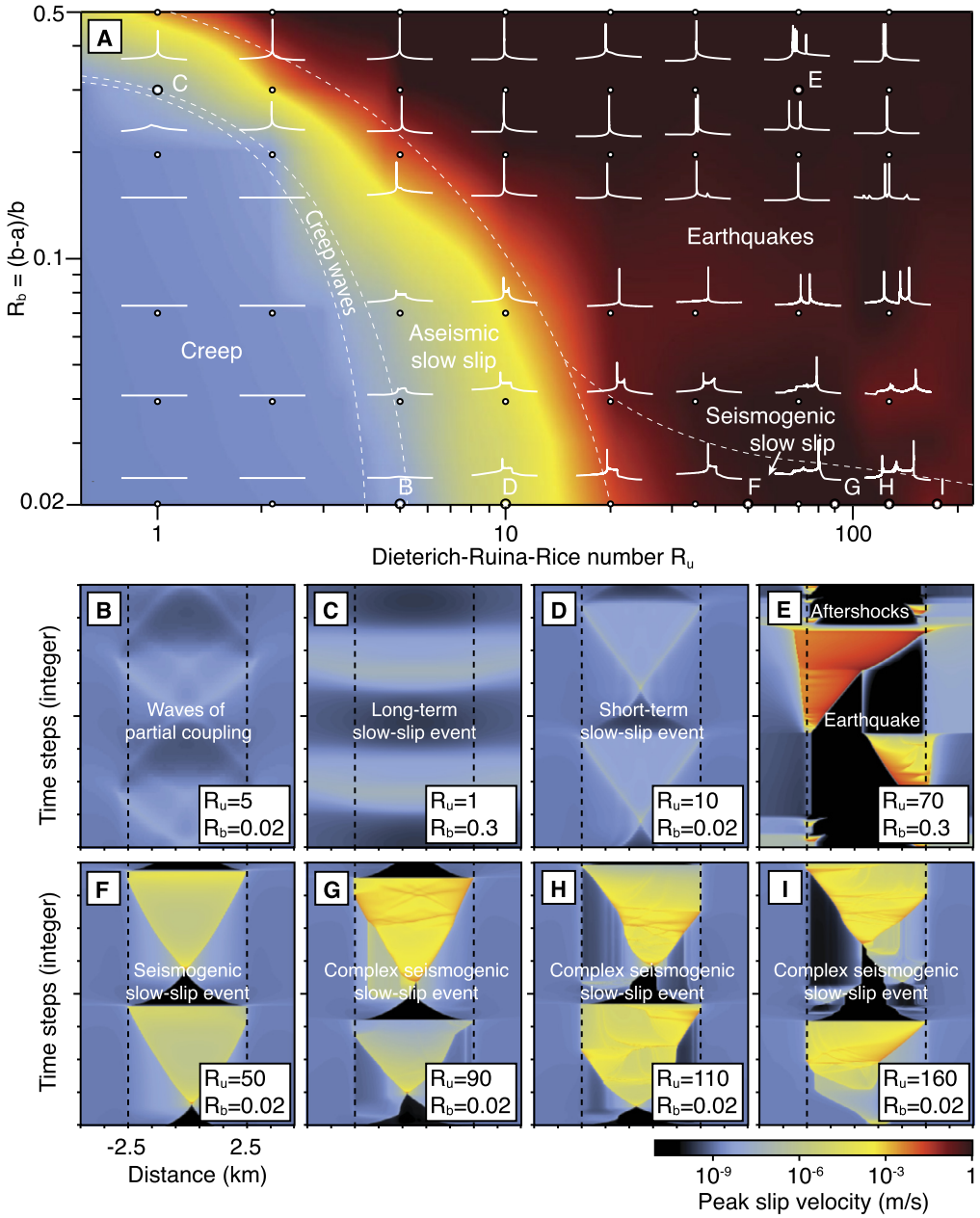

Fig. 2. Seismic cycle simulations under variable R_b and R_u. A) Sub-domains for creep, creep waves, earthquakes, aseismic and seismogenic slow-slip events. The background color indicates the peak slip velocity. The white curves show the time series of peak slip velocities for a one or more events, with varying time scales. B to E) Examples of waves of partial coupling, aseismic slow-slip from low R_u velocity-weakening regime, aseismic slow-slip from medium R_u velocity-neutral regime, and earthquakes. F to I) Seismogenic slow-slip events from high R_u in the near-neutral velocity-weakening regime. The R_u number is controlled by the characteristic weakening distance. The velocity weakening area is between the two dashed lines. The segmentation lines in A) are only conceptual.

millimeters, which is typical for geodetic observations of slow-slip events (e.g., Rogers and Dragert, 2003).

We then compute the seismic waveform at the same location of the geodetic station. We assume a homogeneous full elastic space using a closed-form analytical solution (Pujol, 2003). The near-, intermediate-, and far-field components of the seismic waveforms each correspond to various different linear combinations of the moment-rate and its integrals, with weights depending on the distance and azimuths from source to receiver and arrival times corresponding to S- and P-wave speeds. We assume a rigidity of 30 MPa, a Poisson's ratio of $\nu = 0.25$, and a density of 2800 kg/m^3. We ignore seismic attenuation. We first produce the displacement waveforms. Then, we evaluate a time derivative to obtain the velocity waveforms. In our two-dimensional model, the moment-rate per unit length is a simulation outcome. To propagate the seismic wave in a three-dimensional space, we assume a constant width of 5 km for the source. These assumptions affect the amplitude of the waveforms, but not the phase nor the arrival times. We resample the moment-rate function on the fault at 1 Hz for the entire time series (5.4 years) to reduce the computational cost. This frequency is high enough to sample tremor-like events, avoid severe aliasing, and capture the seismic activity from impulsive signals. The station location to the east of the fault results in only shear waves to be detected.

Each slow-slip event includes seismic activity, and most of the fast events are within slow-slip events (Fig. 5b). Some of these fast events can be distinguished as isolated events, but others are concentrated and difficult to distinguish separately, reflecting the

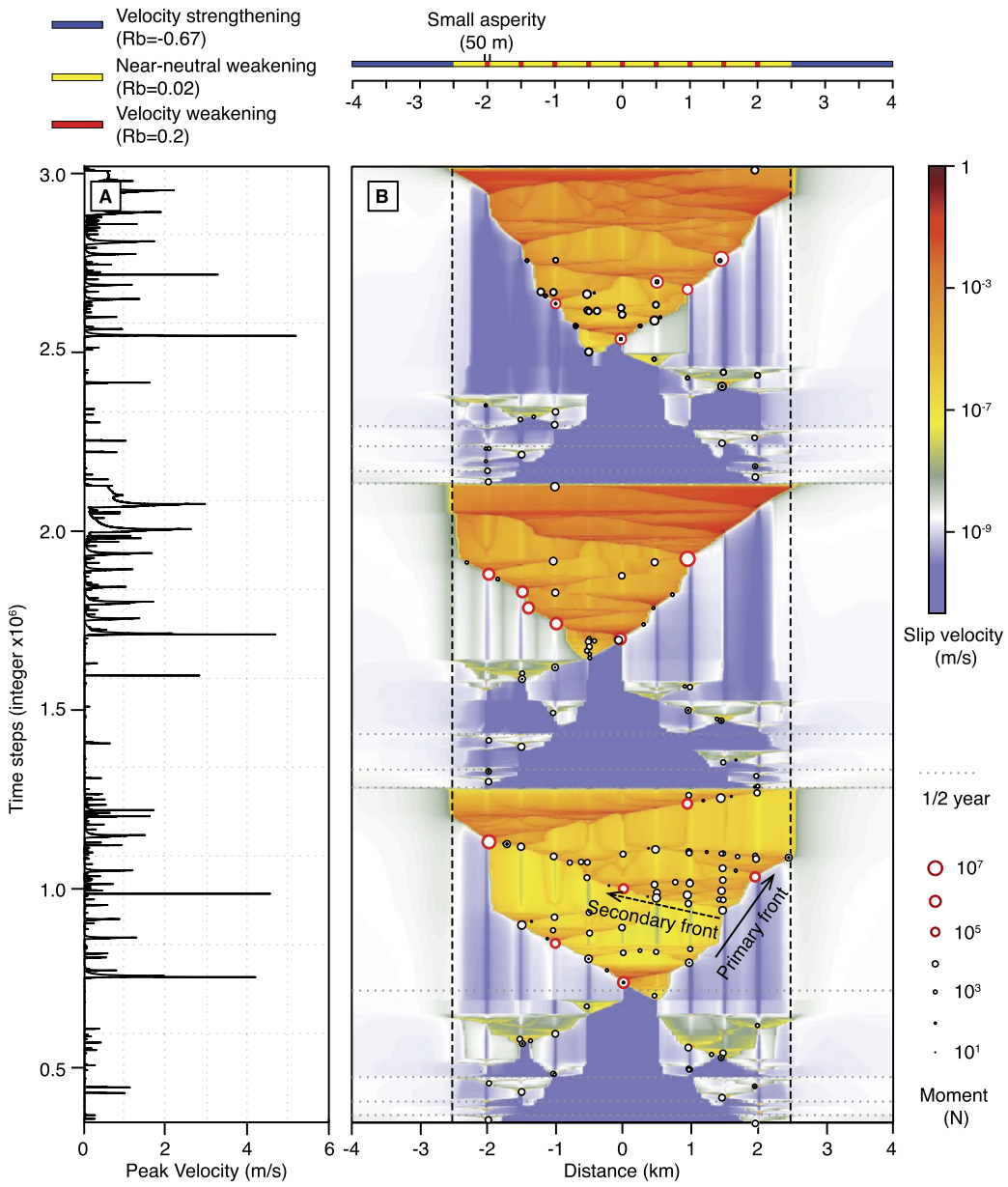

Fig. 3. Simulated collocated fast and slow-slip events with a 2D heterogeneous model. A) Peak velocity of the slip cycles. B) Synthetic slip cycles along the entire fault length. The velocity-weakening area is located between the two vertical black dashed lines. The hypocenters of the seismic events (circles with size scaled by seismic moment) are plotted on top of slip velocity of the rupture cycle.

temporal and spatial clustering of the seismic source (Fig. 4). The slow-slip events that consist of multiple acceleration phases in the geodetic time series are associated with more seismic activity. We compute the seismic waveforms at 16 stations aligned along a fixed azimuthal angle (Fig. 5a) to test whether the body-wave arrivals can be identified. We focus on a single event and we sample the synthetic seismograms at 10,000 Hz to further eliminate aliasing. Unlike the seismo-geodetic station that receives only S waves, these additional seismic stations have an azimuthal angle of 30 degrees, so that both P and S waves can be detected. The arrival of both P and S waves and the moveout pattern is apparent for some of the early phases (Fig. 5c). However, the body-wave arrivals of individual events within rapid bursts of seismicity are intermingled.

The concurrency of seismic and aseismic slip and the clustering of individual fast slip events along slow-slip rupture fronts in our simulations indicate that slow slip triggers small earthquakes and that tremor-like seismic waveforms can be obtained by superposition of the seismic waves radiated by short bursts of small earthquakes. Our simulations imply that seismic and slow-slip events are deeply coupled by the presence of heterogeneous frictional properties within the parametric regime of seismogenic slow-slip. Complex seismogenic slow-slip events emerge spontaneously with a succession of either isolated slow earthquakes or tremors associated with rapid bursts of seismic sources.

5. Discussion

Slow-slip events emerge spontaneously in the framework of rate- and state-dependent friction when the rupture is limited to the nucleation region (Kato, 2003; Lapusta and Rice, 2003; Liu and Rice, 2005, 2007; Rubin, 2008). However, this explanation for slow-slip events in nature is unsatisfactory for two key reasons. First, the parameter space that produces this behavior is so limited that it is unlikely to explain the slow-slip phenomenon in diverse tectonic settings. This realization pushed several investigators to consider

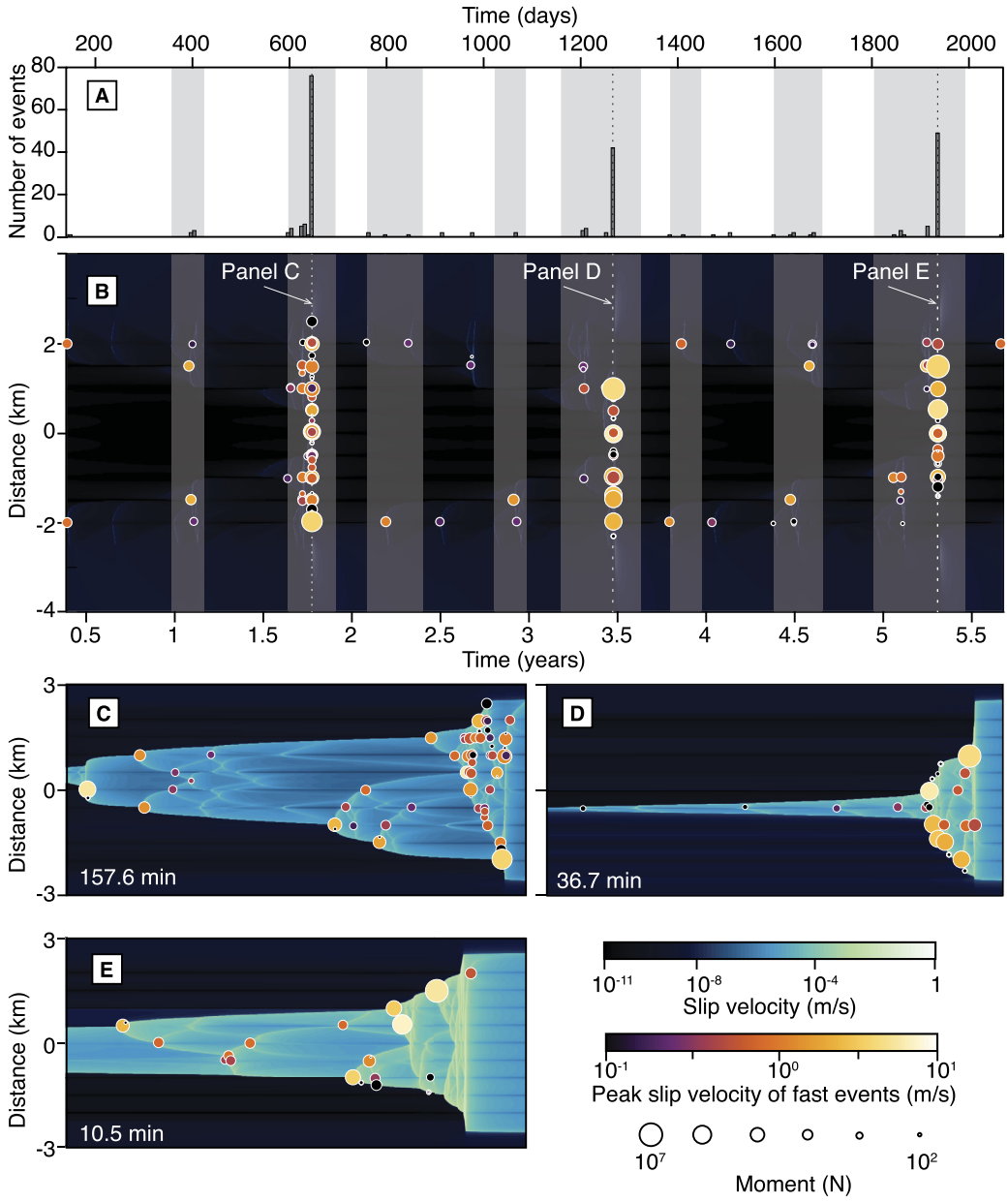

Fig. 4. Space-time distribution of seismic hypocenters for the entire simulation period. A) Histograms of daily slow earthquakes. B) The time distribution of slow (gray bands) and fast (circles scaled by seismic moment and colored by peak velocity) events. The slow-slip events are detected by the average velocity (10^{-6} as the start of a event and 5×10^{-9} as the end) with a duration longer than 60 days. Slow-slip events generally last longer than the seismogenic period, and most seismicity occurs during an underlying slow-slip episode. C) to E) enlarge the three seismogenic periods shown by the dashed lines in figure B). The background color indicates the slip velocity.

coupling with other mechanisms or different friction laws (e.g., Liu and Rubin, 2010; Rubin, 2011, and references therein). Second, the slow-slip events produced in this parameter range are aseismic, failing to explain the strong coupling between slow slip and slow earthquakes observed in nature (e.g., Hall et al., 2019; Hutchison, 2020; Bartlow, 2020, and references therein). In this study, we show that seismogenic slow-slip events are also a spontaneous behavior of rate- and state-dependent friction faults and that the parameter space producing this behavior is essentially unbounded, allowing an arbitrarily small characteristic weakening distance or, equivalently, an arbitrarily small characteristic nucleation size, as long as the rate dependence approaches velocity neutral.

The physical conditions amenable to seismogenic slow-slip events are those found below the seismogenic zone, near the transition between velocity-weakening and velocity-strengthening rate-dependence of steady state friction. We propose that concurrent slow-slip events and slow earthquakes can be explained by a region with nearly velocity-neutral properties, also characterized by a relatively short characteristic nucleation size. The model is appealing because the transition to a velocity neutral rate-dependence is a necessary condition at the boundary of the seismogenic zone, regardless of tectonic setting (Fig. 6). The model explains the underlying mechanism and location of seismogenic slow-slip events up-dip and down-dip of the seismogenic zones at subduction megathrusts. However, the model requires that the boundary spread over several kilometers. In a subduction setting, the down-dip boundary may be accommodated by fluid-assisted regional metamorphism that forms rocks with weakly velocity-weakening properties at high temperature, such as antigorite-rich serpentinite (Shi et al., 2020). The up-dip boundary may correspond to poorly consolidated clay-rich sediments that also exhibit weakly unstable friction (Barbot, 2020). That the Sunda and the

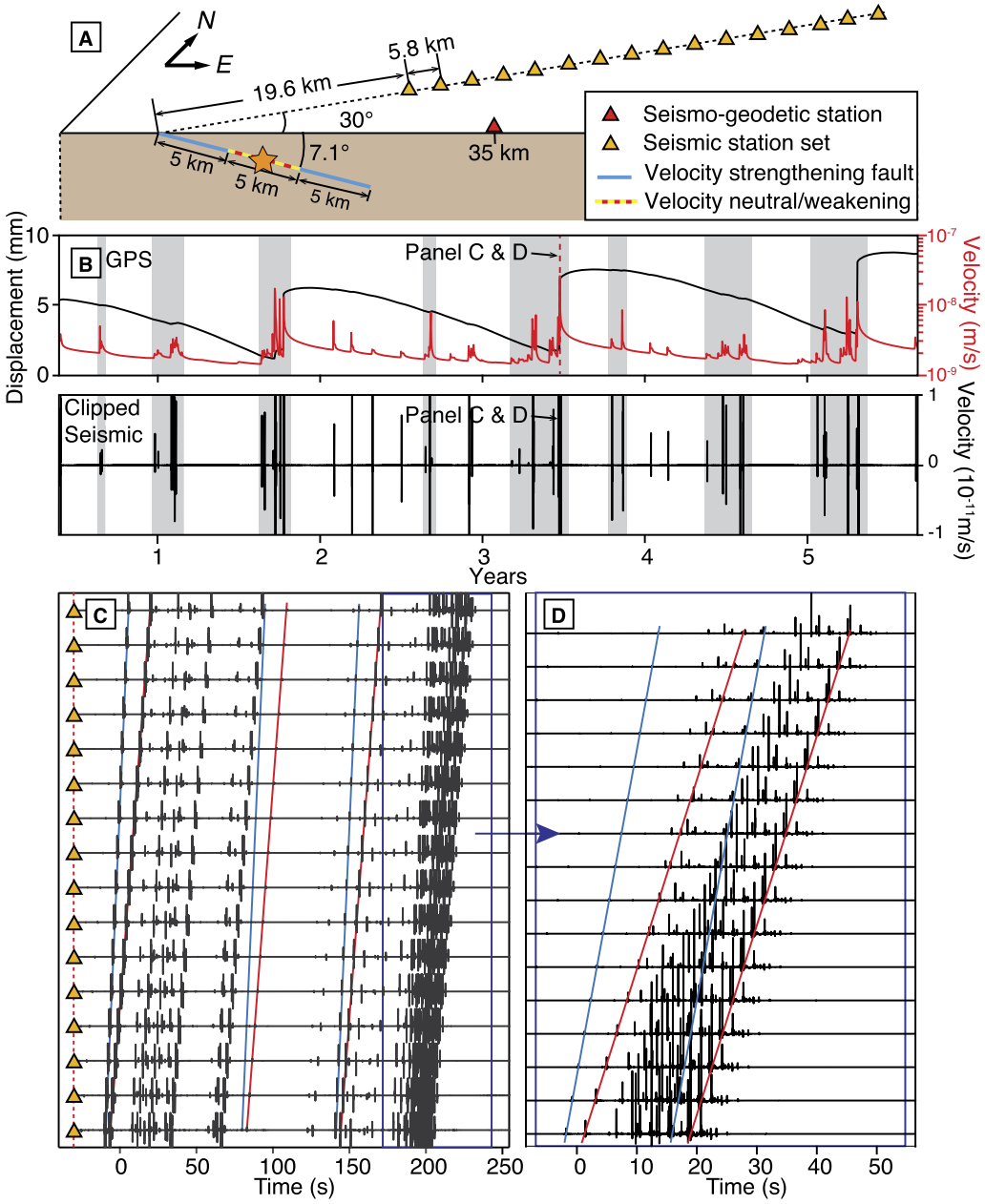

Fig. 5. Geodetic and seismic signatures of seismogenic slow slip. A) Location of the geodetic and seismic receivers relative to the source fault. The source is simplified as a point located in the middle of the velocity-weakening area (orange star). The red triangle indicates the primary station used to simulate geodetic and seismic data for the time series in B). The yellow triangles represent a seismic array with 16 receivers along the same azimuth. B) Synthetic geodetic displacement and velocity (upper panel) and clipped seismograms showing the ground velocity (bottom panel) for the entire sequence. C) Seismograms generated by ruptures highlighted in Fig. 4D and recorded by the orange seismic array in A). The start time is labeled by dashed red line in B). The P and S wave arrivals are marked by the blue and red lines, respectively. D) is the seismograms highlighted by the blue rectangle in C) with a smaller amplitude range.

Japan trenches do not exhibit deep slow-slip events or tremors may be due to an under-developed, i.e., sharp, stability transition or recent giant earthquakes shutting down the slow-slip cycles for a few decades (Shi et al., 2020; Barbot, 2020). Slow-slip and tremors are less frequently observed at continental transforms, and have overall smaller dimensions. However, mixtures of talc and serpentinite in quartz-rich gouge at mid- and lower-crustal depths may provide the conditions for seismogenic slow slip in this context (Moore and Lockner, 2008, 2011).

We highlight the importance of the aseismic and seismogenic end-members of slow-slip events associated with different frictional parameter regimes. Aseismic slow-slip events recur in a more characteristic manner whereas the seismogenic slow-slip events tend to follow a more chaotic cycle. In the seismogenic slow-slip parameter regime, the slow-slip cycle is aperiodic, with large variability of event size, duration, and recurrence time. The ruptures are also more complex, with up-dip and down-dip migrations of the rupture front, marked by similar propagation patterns of seismic sources in the presence of material heterogeneities. The aseismic and seismogenic slow-slip end-members may be used to explain the difference between so-called long-term and short-term slow-slip events in the Nankai Trough, the later being more tremorgenic than the former (Shi et al., 2020). The tremorgenic potential of slow-slip events may be controlled by the concentration of small-scale heterogeneities.

Other mechanisms have been proposed to explain tremors, for example, small-scale geometrical heterogeneity (Tsai and Hirth, 2020) or stress perturbation by fluid migration and metamor-

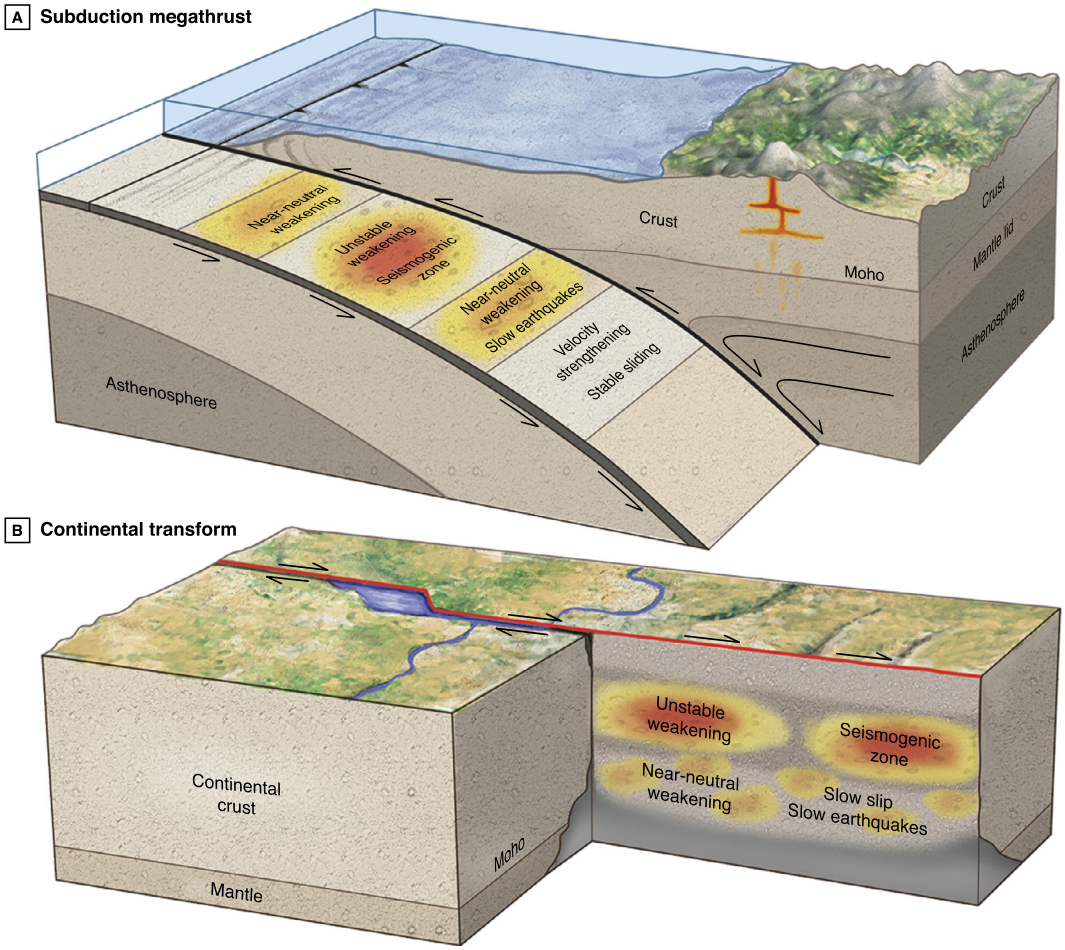

Fig. 6. Schematic distribution of frictional properties on subduction megathrust and continental transform faults. A) Subduction megathrust. The seismogenic zone spans the unstable weakening fault region. Seismogenic slow-slip events take place above and below, in the near-neutral weakening region. B) Continental transform. The seismogenic zone and the seismogenic slow-slip area are associated with unstable weakening and near-neutral weakening friction properties, respectively.

phism (Platt et al., 2018). Given the ample evidence for complexity of exhumed fault zones (e.g., Kotowski and Behr, 2019; Barnes et al., 2020; Kirkpatrick et al., 2021), the role of heterogeneity is important. Recent studies feature fast sub-events by including small scale heterogeneities explicitly (e.g., Luo and Ampuero, 2018; Luo and Liu, 2019), but the detail of the fast ruptures and how they affect the slow-slip propagation is not fully resolved numerically. As seismogenic slow slip may readily be obtained in a homogeneous region with properties systematically found below the seismogenic zone, resolving the effects of heterogeneities may be key to explain the characteristics of tremors, such as the stationary location of tremor hotspots (Rubin and Armbruster, 2013) and rapid tremor migration in the up-dip and down-dip directions (Peng et al., 2015; Peng and Rubin, 2017; Shelly et al., 2007a; Houston et al., 2011).

6. Conclusions

Our study shows that the frictional conditions found near the boundary of the seismogenic zone naturally promote the emergence of slow-slip events for a wide range of frictional properties. Slow-slip events can be categorized by the aseismic and seismogenic end-members depending on the frictional regime, perhaps best exemplified in nature by the long-term and short-term slow-slip events at the Nankai Trough. Aseismic slow-slip events occur when the rupture propagation is limited by the overall size of the asperity and feature a more characteristic cycle. Seismogenic slow-slip events occur in conditions of near-neutral velocity-weakening friction at steady state and feature a more complex, aperiodic sequence, due to the strong coupling between slow slip and embedded fast ruptures. The range of frictional properties for seismogenic slow slip is conceptually unbounded, allowing an arbitrarily small characteristic nucleation size, as long as the rate-dependence approaches velocity-neutral.

The velocity-neutral rate-dependence of friction at steady state occurs systematically near the boundary of the seismogenic zone. The development of slow slip and slow earthquakes depends on the width of this transition and the characteristic nucleation size: Aseismic and seismogenic slow-slip events occur for large and small nucleation sizes, respectively. The width of the stability transition is likely controlled in nature by the down-dip stratification of metamorphic rocks and the properties of the fault zone.

Tremorgenic slow-slip events can occur when small-scale asperities are embedded within a near-neutral velocity-weakening fault. Tremors can result from the rapid succession of clustered seismic sources when the front of slow-slip ruptures passes through these asperities. Rapid tremor reversals (e.g., Ghosh et al., 2010; Houston et al., 2011; Hawthorne et al., 2016) follow from the up-dip and down-dip migrations of the slow-slip rupture front. These results explain the ubiquity of tremorgenic slow-slip events below the seismogenic zone in various tectonic settings. The range of frictional parameters leading to both seismogenic or and tremorgenic slow ruptures is much wider than for aseismic slow-slip events, explaining the predominance of episodic tremor and slip as a slow-slip rupture style in nature.

CRediT authorship contribution statement

Conception and design of study: Shiying Nie, Sylvain Barbot; analysis of data: Shiying Nie; drafting the manuscript: Shiying Nie, Sylvain Barbot.

Declaration of competing interest

We wish to confirm that there are no known conflicts of interest associated with this publication.

Acknowledgements

We thank Pr. Allan Rubin for his valuable suggestions on model construction and two anonymous reviewers for their constructive comments that improved the manuscript. The study benefited from funding from the National Science Foundation, under award number EAR-1848192.

Appendix A. Supplementary material

Supplementary material related to this article can be found online at https://doi.org/10.1016/j.epsl.2021.117037.

References

Audet, P., Bostock, M.G., Christensen, N.I., Peacock, S.M., 2009. Seismic evidence for overpressured subducted oceanic crust and megathrust fault sealing. Nature 457 (7225), 76–78.

Barbot, S., 2019a. Modulation of fault strength during the seismic cycle by grain-size evolution around contact junctions. Tectonophysics 765, 129–145.

Barbot, S., 2019b. Slow-slip, slow earthquakes, period-two cycles, full and partial ruptures, and deterministic chaos in a single asperity fault. Tectonophysics 768, 228171.

Barbot, S., 2020. Frictional and structural controls of seismic super-cycles at the Japan trench. Earth Planets Space 72 (63). https://doi.org/10.1186/s40623-020-01185-3.

Barbot, S., 2021. A spectral boundary-integral method for quasi-dynamic ruptures of multiple parallel faults. Bull. Seismol. Soc. Am. https://doi.org/10.1785/0120210004.

Barbot, S., Lapusta, N., Avouac, J.P., 2012. Under the hood of the earthquake machine: towards predictive modeling of the seismic cycle. Science 336 (6082), 707–710. https://doi.org/10.1126/science.1218796.

Barnes, P.M., Wallace, L.M., Saffer, D.M., Bell, R.E., Underwood, M.B., Fagereng, A., et al., 2020. Slow slip source characterized by lithological and geometric heterogeneity. Sci. Adv. 6 (13), eaay3314. https://doi.org/10.1126/sciadv.aay3314.

Bartlow, N.M., 2020. A long-term view of episodic tremor and slip in Cascadia. Geophys. Res. Lett. 47 (3), e2019GL085303. https://doi.org/10.1029/2019GL085303.

Bell, R., Sutherland, R., Barker, D.H., Henrys, S., Bannister, S., Wallace, L., Beavan, J., 2010. Seismic reflection character of the Hikurangi subduction interface, New Zealand, in the region of repeated Gisborne slow slip events. Geophys. J. Int. 180 (1), 34–48.

Bernaudin, M., Gueydan, F., 2018. Episodic tremor and slip explained by fluid-enhanced microfracturing and sealing. Geophys. Res. Lett. 45 (8), 3471–3480. https://doi.org/10.1029/2018GL077586.

Beroza, G.C., Ide, S., 2011. Slow earthquakes and nonvolcanic tremor. Annu. Rev. Earth Planet. Sci. 39, 271–296.

Bhattacharya, P., Viesca, R.C., 2019. Fluid-induced aseismic fault slip outpaces pore-fluid migration. Science 364 (6439), 464–468. https://doi.org/10.1126/science.aaw7354.

Biemiller, J., Lavier, L., 2017. Earthquake supercycles as part of a spectrum of normal fault slip styles. J. Geophys. Res., Solid Earth 122 (4), 3221–3240.

Blanpied, M.L., Lockner, D., Byerlee, J., 1991. Fault stability inferred from granite sliding experiments at hydrothermal conditions. Geophys. Res. Lett. 18 (4), 609–612.

Blanpied, M.L., Lockner, D.A., Byerlee, J.D., 1995. Frictional slip of granite at hydrothermal conditions. J. Geophys. Res., Solid Earth 100 (B7), 13045–13064.

Blanpied, M.L., Tullis, T.E., Weeks, J.D., 1998. Effects of slip, slip rate, and shear heating on the friction of granite. J. Geophys. Res., Solid Earth 103 (B1), 489–511.

Bletery, Q., Nocquet, J.-M., 2020. Slip bursts during coalescence of slow slip events in Cascadia. Nat. Commun. 11 (1), 1–6.

Boettcher, M.S., Hirth, G., Evans, B., 2007. Olivine friction at the base of oceanic seismogenic zones. J. Geophys. Res. 112 (B1), 13. https://doi.org/10.1029/2006JB004301.

Cattania, C., 2019. Complex earthquake sequences on simple faults. Geophys. Res. Lett. 46 (17–18), 10384–10393. https://doi.org/10.1029/2019GL083628.

Chamberlain, C.J., Shelly, D.R., Townend, J., Stern, T.A., 2014. Low-frequency earthquakes reveal punctuated slow slip on the deep extent of the Alpine Fault, New Zealand. Geochem. Geophys. Geosyst. 15 (7), 2984–2999.

Cruz-Atienza, V.M., Villafuerte, C., Bhat, H.S., 2018. Rapid tremor migration and pore-pressure waves in subduction zones. Nat. Commun. 9 (1), 1–13.

Dragert, H., Wang, K., James, T.S., 2001. A silent slip event on the deeper Cascadia subduction interface. Science 292 (5521), 1525–1528.

Dublanchet, P., 2017. The dynamics of earthquake precursors controlled by effective friction. Geophys. J. Int. 212 (2), 853–871.

Dublanchet, P., Bernard, P., Favreau, P., 2013. Interactions and triggering in a 3-D rate-and-state asperity model. J. Geophys. Res. 118 (5), 2225–2245.

Frank, W.B., Shapiro, N.M., Husker, A.L., Kostoglodov, V., Bhat, H.S., Campillo, M., 2015. Along-fault pore-pressure evolution during a slow-slip event in Guerrero, Mexico. Earth Planet. Sci. Lett. 413, 135–143.

Frank, W.B., Shapiro, N.M., Kostoglodov, V., Husker, A.L., Campillo, M., Payero, J.S., Prieto, G.A., 2013. Low-frequency earthquakes in the Mexican Sweet Spot. Geophys. Res. Lett. 40 (11), 2661–2666. https://doi.org/10.1002/grl.50561.

Fukuyama, E., Tsuchida, K., Kawakata, H., Yamashita, F., Mizoguchi, K., Xu, S., 2018. Spatiotemporal complexity of 2-D rupture nucleation process observed by direct monitoring during large-scale biaxial rock friction experiments. Tectonophysics 733, 182–192.

Gabriel, A.-A., Ampuero, J.-P., Dalguer, L.A., Mai, P.M., 2012. The transition of dynamic rupture styles in elastic media under velocity-weakening friction. J. Geophys. Res. 117 (B9).

Gao, X., Wang, K., 2017. Rheological separation of the megathrust seismogenic zone and episodic tremor and slip. Nature 543 (7645), 416–419.

Ghosh, A., Vidale, J.E., Sweet, J.R., Creager, K.C., Wech, A.G., Houston, H., Brodsky, E.E., 2010. Rapid, continuous streaking of tremor in Cascadia. Geochem. Geophys. Geosyst. 11 (12).

Goswami, A., Barbot, S., 2018. Slow-slip events in semi-brittle serpentinite fault zones. Sci. Rep. 8 (1), 1–11.

Hall, K., Schmidt, D., Houston, H., 2019. Peak tremor rates lead peak slip rates during propagation of two large slow earthquakes in Cascadia. Geochem. Geophys. Geosyst. 20 (11), 4665–4675. https://doi.org/10.1029/2019GC008510.

Hauksson, E., 2011. Crustal geophysics and seismicity in southern California. Geophys. J. Int. 186 (1), 82–98. https://doi.org/10.1111/j.1365-246X.2011.05042.x.

Hawthorne, J.C., Bostock, M.G., Royer, A.A., Thomas, A.M., 2016. Variations in slow slip moment rate associated with rapid tremor reversals in Cascadia. Geochem. Geophys. Geosyst. 17 (12), 4899–4919. https://doi.org/10.1002/2016GC006489.

Hayes, G.P., Moore, G.L., Portner, D.E., Hearne, M., Flamme, H., Furtney, M., Smoczyk, G.M., 2018. Slab2, a comprehensive subduction zone geometry model. Science 362 (6410), 58–61. https://doi.org/10.1126/science.aat4723.

Houston, H., Delbridge, B.G., Wech, A.G., Creager, K.C., 2011. Rapid tremor reversals in Cascadia generated by a weakened plate interface. Nat. Geosci. 4 (6), 404–409. https://doi.org/10.1038/ngeo1157.

Hutchison, A.A., 2020. Inter-episodic tremor and slip event episodes of quasi-spatiotemporally discrete tremor and very low frequency earthquakes in Cascadia suggestive of a connective underlying, heterogeneous process. Geophys. Res. Lett. 47 (3), e2019GL086798. https://doi.org/10.1029/2019GL086798.

Idehara, K., Yabe, S., Ide, S., 2014. Regional and global variations in the temporal clustering of tectonic tremor activity. Earth Planets Space 66 (1), 66. https://doi.org/10.1186/1880-5981-66-66.

Im, K., Saffer, D., Marone, C., Avouac, J.-P., 2020. Slip-rate-dependent friction as a universal mechanism for slow slip events. Nat. Geosci. 13 (10), 705–710. https://doi.org/10.1038/s41561-020-0627-9.

Jolivet, R., Frank, W., 2020. The transient and intermittent nature of slow slip. AGU Adv. 1 (1), e2019AV000126. https://doi.org/10.1029/2019AV000126.

Kaneko, Y., Ampuero, J.-P., 2011. A mechanism for preseismic steady rupture fronts observed in laboratory experiments. Geophys. Res. Lett. 38 (21).

Kato, N., 2003. Repeating slip events at a circular asperity: numerical simulation with a rate- and state-dependent friction law. Bull. Earthq. Res. Inst. Univ. Tokyo 78, 151–166.

Kim, M.J., Schwartz, S.Y., Bannister, S., 2011. Non-volcanic tremor associated with the March 2010 Gisborne slow slip event at the Hikurangi subduction margin, New Zealand. Geophys. Res. Lett. 38 (14). https://doi.org/10.1029/2011GL048400.

Kirkpatrick, J.D., Fagereng, Å., Shelly, D.R., 2021. Geological constraints on the mechanisms of slow earthquakes. Nat. Rev. Earth Environ., 1–17. https://doi.org/10.1038/s43017-021-00148-w.

Kodaira, S., Iidaka, T., Kato, A., Park, J.-O., Iwasaki, T., Kaneda, Y., 2004. High pore fluid pressure may cause silent slip in the Nankai Trough. Science 304 (5675), 1295–1298.

Kostoglodov, V., Singh, S.K., Santiago, J.A., Franco, S.I., Larson, K.M., Lowry, A.R., Bilham, R., 2003. A large silent earthquake in the Guerrero seismic gap, Mexico. Geophys. Res. Lett. 30 (15). https://doi.org/10.1029/2003GL017219.

Kotowski, A.J., Behr, W.M., 2019. Length scales and types of heterogeneities along the deep subduction interface: insights from exhumed rocks on Syros Island, Greece. Geosphere 15 (4), 1038–1065. https://doi.org/10.1130/GES02037.1.

Lapusta, N., Rice, J.R., 2003. Nucleation and early seismic propagation of small and large events in a crustal earthquake model. J. Geophys. Res. 108 (B4), 2205. https://doi.org/10.1029/2001JB000793.
Lapusta, N., Rice, J.R., BenZion, Y., Zheng, G., 2000. Elastodynamics analysis for slow tectonic loading with spontaneous rupture episodes on faults with rate- and state-dependent friction. J. Geophys. Res. 105 (B10), 23765–23789.
Lavier, L.L., Tong, X., Biemiller, J., 2020. The mechanics of creep, slow slip events and earthquakes in mixed brittle-ductile fault zones. J. Geophys. Res., Solid Earth, e2020JB020325.
Liu, Y., Rice, J.R., 2005. Aseismic slip transients emerge spontaneously in three-dimensional rate and state modeling of subduction earthquake sequences. J. Geophys. Res., Solid Earth 110 (B8).
Liu, Y., Rice, J.R., 2007. Spontaneous and triggered aseismic deformation transients in a subduction fault model. J. Geophys. Res. 112 (B9).
Liu, Y., Rice, J.R., 2009. Slow slip predictions based on granite and gabbro friction data compared to GPS measurements in northern Cascadia. J. Geophys. Res., Solid Earth 114 (B9).
Liu, Y., Rubin, A.M., 2010. Role of fault gouge dilatancy on aseismic deformation transients. J. Geophys. Res. 115 (B10414). https://doi.org/10.1029/2010JB007522.
Luo, Y., Ampuero, J.-P., 2018. Stability of faults with heterogeneous friction properties and effective normal stress. Tectonophysics 733, 257–272. https://doi.org/10.1016/j.tecto.2017.11.006.
Luo, Y., Liu, Z., 2019. Rate-and-state model casts new insight into episodic tremor and slow-slip variability in Cascadia. Geophys. Res. Lett. 46 (12), 6352–6362. https://doi.org/10.1029/2019GL082694.
Magistrale, H., 2002. Relative contributions of crustal temperature and composition to controlling the depth of earthquakes in southern California. Geophys. Res. Lett. 29 (10), 87. https://doi.org/10.1029/2001GL014375.
Masuda, K., Ide, S., Ohta, K., Matsuzawa, T., 2020. Bridging the gap between low-frequency and very-low-frequency earthquakes. Earth Planets Space 72, 1–9.
Matsuzawa, T., Hirose, H., Shibazaki, B., Obara, K., 2010. Modeling short- and long-term slow slip events in the seismic cycles of large subduction earthquakes. J. Geophys. Res., Solid Earth 115 (B12).
McCausland, W., Malone, S., Johnson, D., 2005. Temporal and spatial occurrence of deep non-volcanic tremor: from Washington to northern California. Geophys. Res. Lett. 32 (24).
Michel, S., Gualandi, A., Avouac, J.-P., 2019. Interseismic coupling and slow slip events on the Cascadia megathrust. Pure Appl. Geophys. 176 (9), 3867–3891. https://doi.org/10.1007/s00024-018-1991-x.
Moore, D.E., Lockner, D.A., 2008. Talc friction in the temperature range 25°-400°C: relevance for fault-zone weakening. Tectonophysics 449 (1–4), 120–132. https://doi.org/10.1016/j.tecto.2007.11.039.
Moore, D.E., Lockner, D.A., 2011. Frictional strengths of talc-serpentine and talc-quartz mixtures. J. Geophys. Res. 116 (B1). https://doi.org/10.1029/2010JB007881.
Nadeau, R.M., Dolenc, D., 2005. Nonvolcanic tremors deep beneath the San Andreas Fault. Science 307 (5708), 389.
Nanjundiah, P., Barbot, S., Wei, S., 2020. Static source properties of slow and fast earthquakes. J. Geophys. Res. 125 (12), e2019JB019028. https://doi.org/10.1029/2019JB019028.
Nishimura, T., Matsuzawa, T., Obara, K., 2013. Detection of short-term slow slip events along the Nankai Trough, southwest Japan, using GNSS data. J. Geophys. Res. 118 (6), 3112–3125. https://doi.org/10.1002/jgrb.50222.
Obara, K., Kato, A., 2016. Connecting slow earthquakes to huge earthquakes. Science 353 (6296), 253–257.
Okada, Y., 1985. Surface deformation due to shear and tensile faults in a half-space. Bull. Seismol. Soc. Am. 75 (4), 1135–1154.
Okazaki, K., Katayama, I., 2015. Slow stick slip of antigorite serpentinite under hydrothermal conditions as a possible mechanism for slow earthquakes. Geophys. Res. Lett. 42 (4), 1099–1104. https://doi.org/10.1002/2014GL062735.
Okazaki, K., Katayama, I., Takahashi, M., 2013. Effect of pore fluid pressure on the frictional strength of antigorite serpentinite. Tectonophysics 583, 49–53.
Ong, S.Q., Barbot, S., Hubbard, J., 2019. Physics-based scenario of earthquake cycles on the Ventura Thrust system, California: the effect of variable friction and fault geometry. Pure Appl. Geophys. https://doi.org/10.1007/s00024-019-02111-9.
Ozacar, A.A., Zandt, G., 2009. Crustal structure and seismic anisotropy near the San Andreas Fault at Parkfield, California. Geophys. J. Int. 178 (2), 1098–1104.
Peng, Y., Rubin, A.M., 2016. High-resolution images of tremor migrations beneath the Olympic Peninsula from stacked array of arrays seismic data. Geochem. Geophys. Geosyst. 17 (2), 587–601. https://doi.org/10.1002/2015GC006141.
Peng, Y., Rubin, A.M., 2017. Intermittent tremor migrations beneath Guerrero, Mexico, and implications for fault healing within the slow slip zone. Geophys. Res. Lett. 44 (2), 760–770. https://doi.org/10.1002/2016GL071614.
Peng, Y., Rubin, A.M., Bostock, M.G., Armbruster, J.G., 2015. High-resolution imaging of rapid tremor migrations beneath southern Vancouver Island using cross-station cross correlations. J. Geophys. Res. 120 (6), 4317–4332.
Platt, J.P., Xia, H., Schmidt, W.L., 2018. Rheology and stress in subduction zones around the aseismic/seismic transition. Prog. Earth Planet. Sci. 5 (1), 24.
Pujol, J., 2003. Elastic Wave Propagation and Generation in Seismology. Cambridge University Press.
Qiu, Q., Hill, E.M., Barbot, S., Hubbard, J., Feng, W., Lindsey, E.O., Tapponnier, P., et al., 2016. The mechanism of partial rupture of a locked megathrust: the role of fault morphology. Geology 44 (10), 875–878. https://doi.org/10.1130/G38178.1.
Rice, J.R., 1983. Constitutive relations for fault slip and earthquake instabilities. Pure Appl. Geophys. 21, 443–475. https://doi.org/10.1007/978-3-0348-6608-8_7.
Rice, J.R., Ruina, A.L., 1983. Stability of steady frictional slipping. J. Appl. Mech. 50, 343–349. https://doi.org/10.1115/1.3167042.
Rogers, G., Dragert, H., 2003. Episodic tremor and slip on the Cascadia subduction zone: the chatter of silent slip. Science 300 (5627), 1942–1943.
Romanet, P., Bhat, H.S., Jolivet, R., Madariaga, R., 2018. Fast and slow slip events emerge due to fault geometrical complexity. Geophys. Res. Lett. 45 (10), 4809–4819.
Rousset, B., Bürgmann, R., Campillo, M., 2019a. Slow slip events in the roots of the San Andreas Fault. Sci. Adv. 5 (2), eaav3274.
Rousset, B., Fu, Y., Bartlow, N., Bürgmann, R., 2019b. Week-long and year-long slow slip and tectonic tremor episodes on the south central Alaska megathrust. J. Geophys. Res. 122, 13–392. https://doi.org/10.1029/2019JB018724.
Rubin, A.M., 2008. Episodic slow slip events and rate-and-state friction. J. Geophys. Res. 113 (B11414). https://doi.org/10.1029/2008JB005642.
Rubin, A.M., 2011. Designer friction laws for bimodal slip propagation speeds. Geochem. Geophys. Geosyst. 12 (Q04007). https://doi.org/10.1029/2010GC003386.
Rubin, A.M., Armbruster, J.G., 2013. Imaging slow slip fronts in Cascadia with high precision cross-station tremor locations. Geochem. Geophys. Geosyst. 14 (12), 5371–5392. https://doi.org/10.1002/2013GC005031.
Ruina, A., 1983. Slip instability and state variable friction laws. J. Geophys. Res., Solid Earth 88 (B12), 10359–10370.
Schmidt, D., Gao, H., 2010. Source parameters and time-dependent slip distributions of slow slip events on the Cascadia subduction zone from 1998 to 2008. J. Geophys. Res. 115 (B4). https://doi.org/10.1029/2008JB006045.
Scholz, C.H., 1998. Earthquakes and friction laws. Nature 391, 37–42. https://doi.org/10.1038/34097.
Segall, P., Rubin, A.M., Bradley, A.M., Rice, J.R., 2010. Dilatant strengthening as a mechanism for slow slip events. J. Geophys. Res., Solid Earth 115 (B12).
Shelly, D.R., 2010. Migrating tremors illuminate complex deformation beneath the seismogenic San Andreas Fault. Nature 463 (7281), 648–652.
Shelly, D.R., Beroza, G.C., Ide, S., 2007a. Complex evolution of transient slip derived from precise tremor locations in western Shikoku, Japan. Geochem. Geophys. Geosyst. 8 (10).
Shelly, D.R., Beroza, G.C., Ide, S., 2007b. Non-volcanic tremor and low-frequency earthquake swarms. Nature 446 (7133), 305–307.
Shelly, D.R., Beroza, G.C., Ide, S., Nakamula, S., 2006. Low-frequency earthquakes in Shikoku, Japan, and their relationship to episodic tremor and slip. Nature 442 (7099), 188–191. https://doi.org/10.1038/nature04931.
Shelly, D.R., Hardebeck, J.L., 2010. Precise tremor source locations and amplitude variations along the lower-crustal central San Andreas Fault. Geophys. Res. Lett. 37 (L14301), 5. https://doi.org/10.1029/2010GL043672.
Shi, Q., Barbot, S., Wei, S., Tapponnier, P., Matsuzawa, T., Shibazaki, B., 2020. Structural control and system-level behavior of the seismic cycle at the Nankai Trough. Earth Planets Space 72 (1), 1–31. https://doi.org/10.1186/s40623-020-1145-0.
Shibazaki, B., Shimamoto, T., 2007. Modelling of short-interval silent slip events in deeper subduction interfaces considering the frictional properties at the unstable–stable transition regime. Geophys. J. Int. 171 (1), 191–205.
Shiraishi, K., Yamada, Y., Nakano, M., Kinoshita, M., Kimura, G., 2020. Three-dimensional topographic relief of the oceanic crust may control the occurrence of shallow very-low-frequency earthquakes in the Nankai Trough off Kumano. Earth Planets Space 72, 1–14.
Skarbek, R.M., Rempel, A.W., Schmidt, D.A., 2012. Geologic heterogeneity can produce aseismic slip transients. Geophys. Res. Lett. 39 (21). https://doi.org/10.1029/2012GL053762.
Song, T.-R.A., Helmberger, D.V., Brudzinski, M.R., Clayton, R.W., Davis, P., Pérez-Campos, X., Singh, S.K., 2009. Subducting slab ultra-slow velocity layer coincident with silent earthquakes in southern Mexico. Science 324 (5926), 502–506.
Takagi, R., Obara, K., Maeda, T., 2016. Slow slip event within a gap between tremor and locked zones in the Nankai subduction zone. Geophys. Res. Lett. 43 (3), 1066–1074. https://doi.org/10.1002/2015GL066987.
Todd, E.K., Schwartz, S.Y., Mochizuki, K., Wallace, L.M., Sheehan, A.F., Webb, S.C., et al., 2018. Earthquakes and tremor linked to seamount subduction during shallow slow slip at the Hikurangi margin, New Zealand. J. Geophys. Res. 123 (8), 6769–6783. https://doi.org/10.1029/2018JB016136.
Tong, X., Lavier, L.L., 2018. Simulation of slip transients and earthquakes in finite thickness shear zones with a plastic formulation. Nat. Commun. 9 (1), 1–8.
Tsai, V.C., Hirth, G., 2020. Elastic impact consequences for high-frequency earthquake ground motion. Geophys. Res. Lett. 47 (5), e2019GL086302. https://doi.org/10.1029/2019GL086302.
Tse, S.T., Rice, J.R., 1986. Crustal earthquake instability in relation to the depth variation of frictional slip properties. J. Geophys. Res. 91 (B9), 9452–9472.
Veedu, D.M., Barbot, S., 2016. The Parkfield tremors reveal slow and fast ruptures on the same asperity. Nature 532 (7599), 361–365.

Veedu, D.M., Giorgetti, C., Scuderi, M., Barbot, S., Marone, C., Collettini, C., 2020. Bifurcations at the stability transition of earthquake faulting. Geophys. Res. Lett., e2020GL087985. https://doi.org/10.1029/2020GL087985.

Viesca, R.C., 2016a. Self-similar slip instability on interfaces with rate- and state-dependent friction. Proc. R. Soc. A 472 (2192), 20160254.

Viesca, R.C., 2016b. Stable and unstable development of an interfacial sliding instability. Phys. Rev. E 93 (6), 060202.

Wang, L., Barbot, S., 2020. Excitation of San Andreas tremors by thermal instabilities below the seismogenic zone. Sci. Adv., eabb2057. https://doi.org/10.1126/sciadv.abb2057.

Wech, A., Boese, C., Stern, T., Townend, J., 2012. Tectonic tremor and deep slow slip on the Alpine Fault. Geophys. Res. Lett. 39 (10).

Wei, M., Kaneko, Y., Liu, Y., McGuire, J.J., 2013. Episodic fault creep events in California controlled by shallow frictional heterogeneity. Nat. Geosci. 6 (7), 566.

Wu, Y., Chen, X., 2014. The scale-dependent slip pattern for a uniform fault model obeying the rate- and state-dependent friction law. J. Geophys. Res. 119 (6), 4890–4906. https://doi.org/10.1002/2013JB010779.

Yabe, S., Ide, S., 2018. Variations in precursory slip behavior resulting from frictional heterogeneity. Prog. Earth Planet. Sci. 5 (1), 1–11. https://doi.org/10.1186/s40645-018-0201-x.

Yokota, Y., Ishikawa, T., Watanabe, S.-i., Tashiro, T., Asada, A., 2016. Seafloor geodetic constraints on interplate coupling of the Nankai Trough megathrust zone. Nature 534 (7607), 374–377.

Zigone, D., Rivet, D., Radiguet, M., Campillo, M., Voisin, C., Cotte, N., et al., 2012. Triggering of tremors and slow slip event in Guerrero, Mexico, by the 2010 Mw 8.8 Maule, Chile, earthquake. J. Geophys. Res. 117 (B9). https://doi.org/10.1029/2012JB009160.